9578 *Macromolecules* **2010**, *43*, 9578–9582
DOI: 10.1021/ma1018796

Macromolecules
NOTE

Thermodynamics of TMPC/PSd/Fullerene Nanocomposites: SANS Study

Yang-Choo Chua, Alice Chan, Him-Cheng Wong, Julia S. Higgins, and João T. Cabral*

Department of Chemical Engineering, Imperial College London, London SW7 2AZ, United Kingdom

Received May 17, 2010; Revised Manuscript Received September 7, 2010

ABSTRACT: We report a small angle neutron scattering study of the thermodynamics of a polymer mixture in the presence of nanoparticles, both in equilibrium and during phase separation. Neutron cloud point measurements and random phase approximation (RPA) analysis demonstrate that 1−2 mass % of C_{60} fullerenes destabilizes a highly interacting mixture of poly(tetramethyl bisphenol A polycarbonate) and deuterated polystyrene (TMPC/PSd). We unequivocally corroborate these findings with time-resolved temperature jump experiments that, in identical conditions, result in phase separation for the nanocomposite and stability for the neat polymer mixture. At lower C_{60} loadings (viz. 0.2−0.5 mass %), stabilization of the mixture is observed. The nonmonotonic variation of the spinodal temperature with fullerene addition suggests a competitive interplay of asymmetric component interactions and nanoparticle dispersion. The stability line shift depends critically on particle dispersion and vanishes upon nanoparticle agglomeration.

Introduction

Solid fillers are often added to polymers to reduce their cost and improve performance. In recent years, the use of nanoparticles (NPs) as fillers has become increasingly attractive as evidence shows that trace amounts (∼0.01−1%) of molecularly dispersed particles can dramatically enhance the electrical, optical, permeability and mechanical properties of the polymers.[1,2] The resulting nanocomposites find applications in diverse fields, ranging from organic electronics to membranes and biomaterials. The addition of NPs to polymer mixtures may affect the compatibility of polymer mixtures, as reported experimentally[3−9] and theoretically,[10,11] as well as phase separation mechanisms and kinetics in bulk[12] and thin films.[13−15] Not only do such effects have important implications for the formulation and processing of polymer mixtures but the interplay between the self-assembly of the various components during phase separation may also provide novel routes to the fabrication of functional hybrid materials.[16] In spite of the fundamental and industrial relevance of these materials, relatively few systematic theoretical and experimental studies have investigated the effect of NPs on the thermodynamics of polymer mixtures. Furthermore, thermodynamic studies have previously relied on time-resolved light scattering or cloud point measurements, where the phase boundary was determined from the observation of turbidity indicating the onset of phase separation.[7] Such nonequilibrium measurements, however, depend on dynamic effects (rate, viscosity, mechanism, and separation kinetics) and the observed cloud points generally differ, approximating the equilibrium boundaries to varying extent. A further complication of experimental studies of nanocomposite systems arises from a limited (and time-varying, e.g. during thermal processing) dispersion of NPs in the polymer matrix. Combining small angle neutron scattering (SANS) with light scattering and cloud point measurements, Yurekli et al. have shown that the addition of layered silicates, up to a volume fraction of 0.04, leaves the overall blend phase boundaries essentially unchanged,[3] although the kinetics and morphology of phase separation are altered.[12] Simulations performed by Ginzburg however predict shifts in the location of the spinodal: NPs can either promote or hinder mixing, depending on their size and polymer degree of polymerization, as well as their absolute and relative interactions with the polymer components.[10] Polystyrene/polybutadiene mixtures, for instance, have been found to be destabilized by the addition of fumed silica fillers, which could be reversed upon surface-functionalization of the fillers.[8] Further, nanoparticles have been reported to alter glass formation in polymers, including the glass transition temperature, which can increase or decrease by up to 10 s of degrees, depending on interactions, loading and dispersion in the matrix.[17−21]

In this work, based on SANS study, we report on the thermodynamics of a series of lower critical solution temperature (LCST) mixtures of poly(tetramethyl bisphenol A polycarbonate) and deuterated polystyrene (TMPC/PSd) containing Buckminster fullerenes (C_{60}). The phase behavior of the TMPC/PSd system has been well characterized,[22] and C_{60} can be molecularly dispersed in these polymers matrices at 1−2% mass fraction.[17−19,23−25] Nanocomposites of TMPC/PS with C_{60} are of particular interest because fullerene-polymer blends have wide applications in organic photovoltaics,[26] and TMPC is the only polycarbonate miscible with PS.[27] To the best of our knowledge, this is the first study on the thermodynamics of bulk binary polymer mixtures under the influence of *molecularly dispersed* NPs. By probing the thermodynamics of the mixtures in equilibrium, we eliminate kinetic effects (such as viscosity[24,28,29] or glass transition temperature changes[17−21] induced by the nanoparticles) which can affect the measurement of the phase behavior of the mixtures. Our studies demonstrate that depending on its loading and dispersion, C_{60} fullerenes can stabilize, destabilize or have no effect on the thermodynamics of the near-critical, highly interacting, TMPC/PSd polymer mixture.

Experimental Section

Mixtures of TMPC and PSd of near-critical composition (50/50 mass fraction) and nanocomposites with 0.2, 0.5, 1.0, 2.0, and 4.0 mass % C_{60} were prepared by rapid coprecipitation.[23] C_{60} (MER Corp., 99+% purity) was dissolved to give a 0.1% mass fraction toluene solution (99.8+%, GLC, Fisher Scientific), stirred for 8 h and sonicated (CAMLAB Transsonic T570/H) for 30 min. Separately, TMPC (Bayer, AG) and PSd (Polymer Source) were codissolved in 10% mass fraction toluene solution

*Corresponding author. E-mail: j.cabral@imperial.ac.uk.

 Published on Web 10/28/2010

Table 1. Characteristics of the Polymers under Study[a]

	$\langle M\rangle_w$ (g/mol)	$\langle M\rangle_w/\langle M\rangle_n$	m (g/mol)	b_{coh} (fm)	v (cm^3/mol)	a (Å)	R_g (nm)
PSd	100 300	1.09	112.2	106.54	108.9	6.7	7.8
TMPC	37 450	2.24	310.4	68.07	308.0	20.1	6.0

[a] Weight- and number-average degrees of polymerization, $\langle M\rangle_w$ and $\langle M\rangle_n$ [as reported by the supplier (for PSd standard) and determined by triple detection GPC (for TMPC)]; m is the molecular weight of the monomer unit; b_{coh} is the neutron scattering length of the monomer units; a is the polymer segment length;[22,31] R_g is the number-average radius of gyration; v are average monomer molar volumes as computed from PVT data[32] for the range of temperatures tested [assuming v(PSd) ≈ v(PS)]. The reference volume of the system is defined as $v_0 = (v_{PSd}v_{TMPC})^{1/2}$ and computed to be 183.1 cm^3/mol.

and stirred for 8 h. The two solutions were added, sonicated for 30 min and further stirred for 36 h. The nanocomposite was then precipitated in excess methanol (99.5+%, GLC, Fisher Scientific) forming fiber composites, then dried under vacuum at 100 °C for 1 day and 130 °C (at T_g onset but below agglomeration temperature)[17,18] for 2 days to ensure complete removal of solvents. The dried samples were then hot pressed between Kapton sheets at 185 °C for at least 6 min to form 150−200 μm thick films. Neat TMPC/PSd 50/50 mixtures were prepared by the same method for comparison purposes. Glass transition temperatures were determined by calorimetry (TA Instruments Q2000, 10 °C/min, midpoint method) and found to be 140 ± 4 °C, for the neat TMPC/PSd mixture and nanocomposites, in line with previous reports.[17−19] The characteristics of the polymers are summarized in Table 1. The dispersion of C_{60} in the polymer mixtures was assessed by wide-angle X-ray scattering (WAXS) using a PANalytical X'Pert PRO diffractometer equipped with an X-Celerator detector and Cu anode source (K_α: λ = 1.54 Å). Prior to annealing, no crystalline peaks corresponding to C_{60} crystallization are observable in the nanocomposite indicating nanoparticle dispersion. C_{60} crystalline peaks have been reported in PS nanocomposites above 2 mass % C_{60}.[24,25] In the current TMPC/PSd/C60 nanocomposite, upon annealing above the agglomeration threshold temperature (~T_g + 80 °C[17] for PS, corresponding to a viscosity of 10^5−10^6 Pa s, and approximately 220−235 °C for TMPC/PS 50/50[30]), C_{60} peaks appear in the nanocomposites containing ≥2% C_{60} (Figure 1). C_{60} crystallization in nanocomposites upon annealing was separately determined by cross-polarized microscopy (Olympus BX41M). To evaluate the effect of dispersion and thermal processing in the effective interaction parameter measured by SANS, a "poorly" dispersed 2%-C_{60} composite was prepared by prolonged annealing above the agglomeration threshold temperature.

A custom-made "T-jump" neutron cell,[22] consisting of two brass ovens with quartz windows and a motorized sample carrier, was employed for both equilibrium and phase separation SANS experiments. SANS measurements for equilibrium studies were performed at: (a) PAXE (Laboratoire Léon Brillouin, Saclay) using a neutron wavelength of λ = 15 Å and sample-to-detector distance, $D_{s\text{-}d}$ = 5.11 m, which yields a wavevector range of 0.0033 Å^{-1} < q < 0.048 Å^{-1}, and (b) D11 (Institute Laue-Langevin, Grenoble), with λ = 8 Å and $D_{s\text{-}d}$ = 8 m, yielding 0.007 Å^{-1} < q < 0.063 Å^{-1}; $q = 4\pi/\lambda \sin(\theta/2)$, where θ is the scattering angle. Neutron cloud point and random phase approximation (RPA) measurements were performed in situ at PAXE by loading the sample into the preheated cell at 225 °C, and heating at a rate of 1 °C/min to 280 °C while acquiring data every 60 s; each scan essentially averages the scattering from the sample at ΔT = 1 °C intervals. These (relatively short) scan times are chosen to allow equilibration of the spectrum of concentration fluctuations of the specimens at the measured temperatures and to ensure sufficient statistics while maximizing temperature resolution. Temperature-scanning SANS is possible because of the proximity to the phase boundaries, while still in the mean-field region, and the strong scattering signal of the TMPC/PSd system. To complement the neutron cloud point experiments, isothermal RPA measurements were performed at D11; the samples were annealed in situ in the "T-jump" cell from 170 °C until up to 255 °C, before their scattering was acquired. In both experiments, the centrosymmetric raw spectra were radially averaged, corrected for empty cell scattering and calibrated with a set of secondary

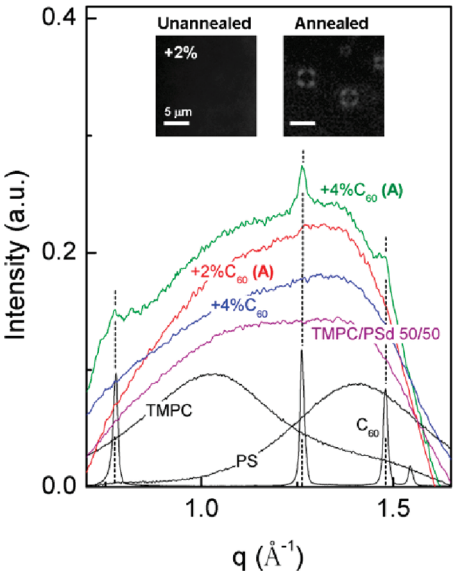

Figure 1. WAXS patterns for C_{60}, PS, TMPC, TMPC/PSd 50/50, and its nanocomposites before and after annealing. No peaks are observed in the nanocomposites before annealing (up to 4 mass %), indicating nanoparticle dispersion. Upon annealing at 235 °C for 15 min, clear C_{60} peaks are observed in the 4 mass % nanocomposite, while 2 mass % nanocomposites exhibit a shoulder at q ~ 1.26 Å^{-1} after prolonged annealing at 235 °C for 6 h. The inset shows the appearance of birefringence in the 2 mass % nanocomposite under cross polarizers after prolonged annealing, indicating the formation of phase-separated C_{60} crystallites.

standards and direct beam. The coherent scattering function was obtained by subtraction of the appropriate volume fraction of the calibrated spectra of the pure components, TMPC and PSd. Sample thicknesses and uncertainty, necessary for absolute intensity calibration, were determined independently with a micrometer (1 μm resolution) as well as from the specimen transmission, and transmission versus thickness calibration curve. Phase separation experiments were further carried out at D11 at lower wavenumbers, with λ = 8 Å and $D_{s\text{-}d}$ = 39 m, providing a q-range of 0.0025 Å^{-1} < q < 0.014 Å^{-1} necessary for such measurements (light scattering is unfeasible due to the small transmission of the specimens). Samples were first preannealed at 235 °C (below the phase boundary) and allowed to equilibrate (for at least 120 s) before they were rapidly quenched to 255 °C. Acquisition times of 5 s (with dead time of 250 ms) were used. Acquisition was synchronized with the final positioning of the sample holder in the "experimental oven" and time set to t = 0 s.

Results and Discussion

Figure 2 plots the cloud point curves (viz. integrated scattering intensities as a function of temperature) for neat TMPC/PSd and the 1 and 2 mass % C_{60} nanocomposites. The curves clearly indicate an earlier onset of intensity rise from the baseline in the nanocomposites, showing that the addition of 1−2 mass % C_{60} lowers the spinodal temperature in the TMPC/PSd mixture. It is however not trivial to locate the spinodal temperature from the integrated intensity curves, as strong scattering from concentration

fluctuations in the one phase (eventually diverging at the spinodal) precedes the onset of phase separation.[33,34]

To examine quantitatively the phase behavior of the mixtures, we employ the random phase approximation (RPA)[34] to fit the scattering data.[22] The structure factor of the mixture, $S(q)$ is expressed in terms of the components' $S_i(q)$ (assuming Schultz−Zimm polydispersity[35,36]) and an effective dimensionless Flory−Huggins interaction parameter $\tilde{\chi}_{12}$ as[34,37]

$$\frac{1}{S(q)} = \frac{1}{S_1(q)} + \frac{1}{S_2(q)} - 2\frac{\tilde{\chi}_{12}}{\nu_o} \quad (1)$$

Scattering from TMPC/PSd/2 mass % C_{60} under isothermal annealing at 220 °C (~1 h) remains unchanged within experimental uncertainty, corroborating the WAXS results that fullerenes remain dispersed in this time range; dispersed C_{60} scattering is effectively matched to the deuterated component and thus eq 1 adequately approximates the scattering of the nanocomposite to a two-component system. In the zero-angle limit, eq 1 yields:

$$\frac{1}{S(0)} = \frac{1}{\phi_1 \nu_1 \langle N_1 \rangle_w} + \frac{1}{\phi_2 \nu_2 \langle N_2 \rangle_w} - 2\frac{\tilde{\chi}_{12}}{\nu_o} \quad (2)$$

where $\langle N_i \rangle_w$ is the number-average degree of polymerization of component i, ϕ_i its volume fraction, and ν_o is a reference molar volume, which is taken as the geometric average of the components volume ν_i ($\nu_o \equiv (\nu_1 \nu_2)^{1/2}$). The susceptibility yields the second derivative of the free energy of mixing with respect to composition, i.e. $1/S(0) = \partial^2 \Delta Gm/\partial \phi^2 \equiv G''$.[34] The low-angle ($qR_g \ll 1$) scattering is described by the usual Ornstein−Zernike Lorentzian profile

$$S(q) = \frac{S(0)}{1 + \xi^2 q^2}$$

which is linear in the Zimm representation as $1/S(q) = 1/S(0) + Aq^2$; the spinodal temperature T_S (where $G'' = 0$) is obtained by extrapolation of the intercept to zero from the one-phase region.

Figure 3 shows the coherent scattering intensity of the mixtures at selected temperatures in the one-phase region obtained from real-time temperature ramp SANS (PAXE). The lines correspond to RPA fits (eq 1), with $\tilde{\chi}_{12}$ as the adjustable parameter; segment lengths determined previously[22] are confirmed by equilibrium RPA measurements and are therefore fixed in temperature-ramp SANS to improve fitting accuracy; the insets show the Ornstein−Zernike fits at small wavenumbers for the corresponding mixtures at selected temperatures. RPA describes all scattering data in the one-phase region and, despite some scatter due to the limited 60 s statistics, Ornstein−Zernike scattering shows parallel lines of constant slope (constant polymer dimensions) and positive intercept (proportional to G''). Kratky plots of all mixtures also exhibit high-q asymptotes in good agreement with previous measurements,[22] indicating no change in polymer conformation within measurement uncertainty.

Figure 4a shows the G'' extracted from the isothermal scattering data over the entire temperature range. $G'' = (2/v_0)[\chi_s - \tilde{\chi}_{12}(T)]$, where χ_s is the interaction parameter at the spinodal. The extrapolation of $G'' \to 0$ directly yields the spinodal temperature (T_s). G'' fits for the neat mixture are consistent with previous data.[22,38] χ is generally parametrized as $\chi = A + B/T$; A is associated with changes in local energetics, while B represents the entropic contribution to χ arising from changes in packing upon mixing.[39,40] Closer inspection of Figure 4a, however, suggests that at higher temperatures, G'' exhibits relatively smaller changes with $1/T$, characteristic of "flat" (i.e., nearly composition-independent) phase diagrams, as is known for TMPC/PSd.[41] Component interactions can then be empirically written as $\chi = A + B/T + C/T^2$ where A and B contain the combinatorial entropic and enthalpic contributions respectively, while the noncombinatorial entropic term C encompasses additional constraints due to monomer architecture, connectivity, finite compressibility and any specific interactions that may cause changes in the monomer free volume or mobility.[42] The accessible RPA temperature range (ΔT = 60−80 °C, bound by T_g and T_s) however precludes a robust determination of A, B, and C in a nonlinear fit. Figure 4a shows that the addition of 1−2 mass %

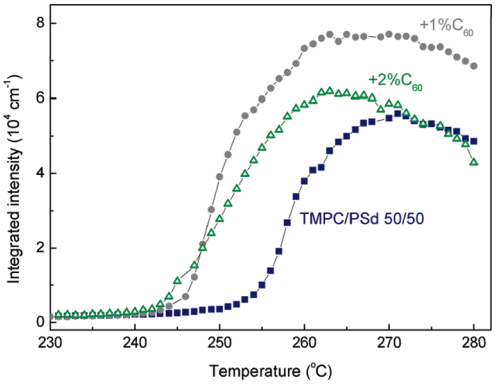

Figure 2. Neutron cloud point curves for TMPC/PSd 50/50, 1, and 2 mass % C_{60} nanocomposites heated at 1 °C/min, obtained by integrating the scattering intensity over the wavevector range 0.0033−0.048 $Å^{-1}$.

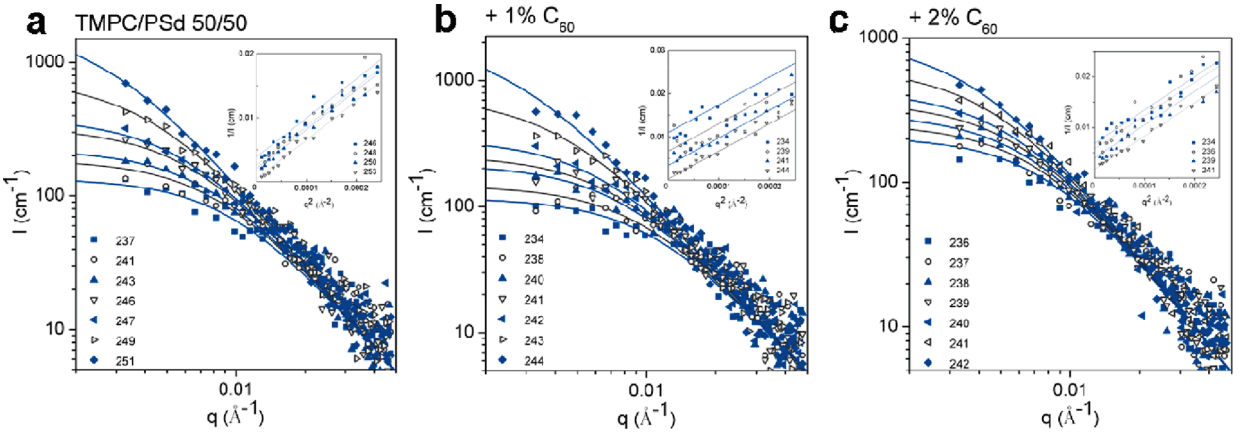

Figure 3. Coherent scattering intensity for (a) TMPC/PSd 50/50 and fullerene nanocomposites with (b) 1 and (c) 2 mass % C_{60} at selected temperatures in the one-phase region. The lines correspond to RPA fits (eq 1). Insets: Ornstein−Zernike fits for the corresponding mixtures at small wavenumbers.

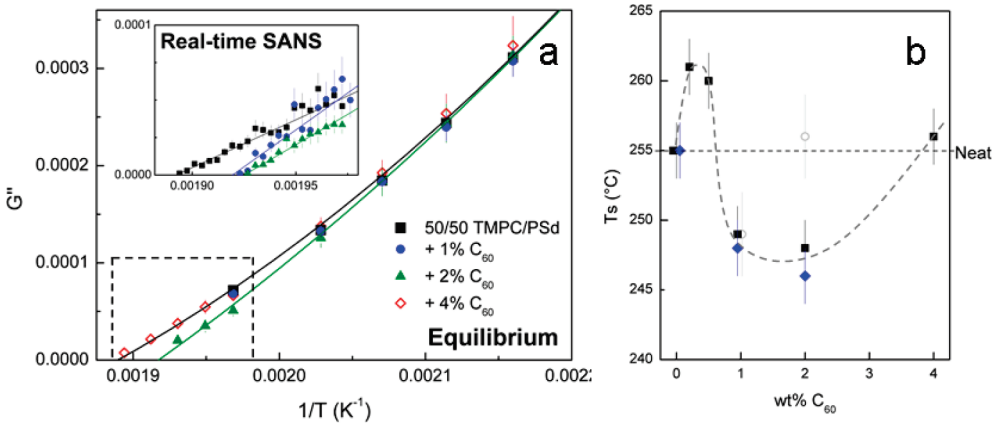

Figure 4. (a) G'' obtained from fits to isothermal and temperature-ramp RPA scattering data. The lines indicate parabolic fits through the data points. Inset: Extrapolation of T_s based on G'' obtained from fits to real-time scattering data in the neutron cloud point experiment; the boxed region indicates the temperature range of the neutron cloud point measurement. (b) T_s as a function of C_{60} loading obtained from the (■) isothermal and (blue ◆) real-time measurements for the dispersed and (○) thermally annealed specimens. The dashed line is a guide to the eye.

C_{60} results in a decrease of T_s for the TMPC/PSd mixture by 7−10 °C. Figure 4b summarizes the variation of T_s with C_{60} content. The results confirm the cloud point curves (Figure 2): namely, that the addition of 1−2 mass % C_{60} lowers the T_s of the TMPC/PSd 50/50 mixture. This destabilization effect depends on the dispersion of the nanoparticles: poorly dispersed composites do not alter T_s within experimental uncertainty. Above a miscibility threshold as observed for 4 mass % C_{60}, or after prolonged annealing, as observed for 2 mass % C_{60} (annealed for 6 h+ above the agglomeration threshold temperature), the neat T_s is recovered. We also observe an increase in the nanocomposite T_s at low loadings of 0.2 and 0.5 mass % C_{60} by ~5 °C. Nonmonotonic variations in ΔT_s have in fact been predicted[43] and observed experimentally[44] in binary mixtures with diblock-copolymers and other additives with competitive interactions. Also, apparent stabilization and destabilization effects in pseudo-binary mixtures can be trivially caused as the critical temperature and composition are generally simultaneously altered by the addition of a third component. Further, the phenomenological "Timmermans mixing rule"[45−47] predicts that additives which are equally soluble in both components of a binary mixture tend to stabilize the mixture (i.e., enlarge the miscibility window), while those with preferential solubility in one component tend to destabilize it. Separate WAXS experiments of TMPC-C_{60} and PS-C_{60} mixtures indicate that C_{60} exhibits slightly better solubility in PS than in TMPC (see Supporting Information). Such preferential interactions could give rise to an asymmetry in binary interactions, sometimes called the "$\Delta\chi$ effect".[48,49] For nanoparticle additives, the relative affinities may further be altered upon aggregation (as miscibility is size-dependent[23] and the overall surface area changes[17]). Variation of fullerene loading and dispersion is expected to alter the extent of enthalpic interactions (both self- and pairwise interactions in the ternary mixture, including $\pi-\pi$ stacking) and entropic contributions ("entropic surface tension" caused by chain stretching in the vicinity of the NPs)[10] within the TMPC and PSd matrices. In particular, as the role of "entropic surface tension" increases as the NP size increases,[10] one can envisage that "small" NPs ($< R_g$) may stabilize the mixture, but destabilize it at higher loading levels (as dispersibility degrades and their effective size increases), due to the larger entropic penalty involved. The nontrivial interplay of competitive interactions and dispersion is thus likely responsible for the nonmonotonic shifts in T_s observed in Figure 4(b).

To validate unequivocally our findings, real-time phase separation experiments were performed. Figure 5 shows the scattering patterns exhibited by the unfilled TMPC/PSd 50/50 mixture and

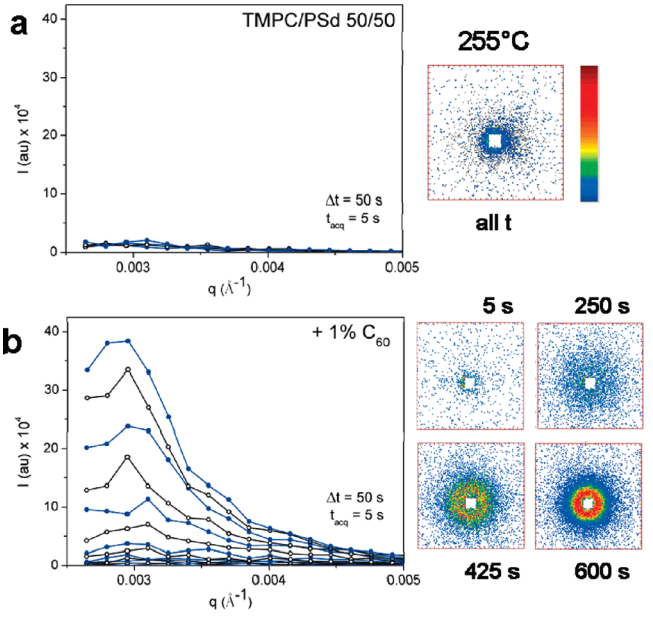

Figure 5. Evolution of the structure factor with time and selected two-dimensional scattering patterns for (a) unfilled TMPC/PSd 50/50 and (b) the +1 mass % C_{60} nanocomposite when heated from the one-phase region to 255 °C. Clear spinodal decomposition is observed in part b, whereas part a shows no signs of phase separation on the experimental time scale.

+1 mass % C_{60} nanocomposite when heated from the one-phase region to 255 °C. Clear spinodal decomposition was observed in the 1% nanocomposite whereas in the unfilled mixture, no phase separation was observed in the experimental time scale.

In summary, we report the destabilization of a near-critical mixture of TMPC/PSd 50/50 by well-dispersed C_{60} fullerenes, manifested by a 7−10 °C reduction of the spinodal temperature at 1−2 mass % loading, based on neutron scattering experiments carried out on both sides of the phase boundary. Beyond a miscibility and/or agglomeration threshold, the T_s of the neat mixture is recovered. Loading of 0.2−0.5 mass % leads to a small increase in T_s. The addition of a third component to a binary polymer mixture has been known to shift both the critical temperature and composition, depending on interaction symmetry. In nanocomposites, such effects are evidently more complex as the component interactions are also sensitive to nanoparticle loading and dispersion. Further composition mapping of the

phase boundaries and critical region, as well as phase separation kinetics, are underway to fully evaluate the impact of nanoparticles in polymer mixture phase behavior.

Acknowledgment. The authors thank the Laboratoire Léon Brillouin (Saclay, France) and Institute Laue-Langevin (ILL) for beamtime, as well as José Teixeira (PAXE), Peter Lindner (ILL) and Ralf Schweins (ILL) for assistance and many useful discussions. Funding from EPSRC and King Abdullah University of Science and Technology (KAUST) is gratefully acknowledged. Y.-C.C. thanks Agency for Science, Technology and Research (A*STAR), Singapore for a postdoctoral fellowship.

Supporting Information Available: Figure showing the miscibility study of TMPC-C_{60} and PS-C_{60} nanocomposites by WAXS. This material is available free of charge via the Internet at http://pubs.acs.org.

References and Notes

(1) Balazs, A. C.; Emrick, T.; Russell, T. P. *Science* **2006**, *314* (5802), 1107–1110.
(2) Paul, D. R.; Robeson, L. M. *Polymer* **2008**, *49* (15), 3187–3204.
(3) Yurekli, K.; Karim, A.; Amis, E. J.; Krishnamoorti, R. *Macromolecules* **2004**, *37* (2), 507–515.
(4) Gharachorlou, A.; Goharpey, F. *Macromolecules* **2008**, *41* (9), 3276–3283.
(5) Si, M.; Araki, T.; Ade, H.; Kilcoyne, A. L. D.; Fisher, R.; Sokolov, J. C.; Rafailovich, M. H. *Macromolecules* **2006**, *39* (14), 4793–4801.
(6) Vo, L. T.; Giannelis, E. P. *Macromolecules* **2007**, *40* (23), 8271–8276.
(7) (a) Lipatov, Y. S. *Prog. Polym. Sci.* **2002**, *27* (9), 1721–1801. (b) Lipatov, Y. S. *J. Macromol. Sci., Part B: Phys.* **2006**, *45* (5), 871–888. (c) Lipatov, Y. S.; Nesterov, A. E.; Ignatova, T. D.; Nesterov, D. A. *Polymer* **2002**, *43* (3), 875–880. (d) Lipatov, Y. S.; Nesterov, A. E. *Polym. Eng. Sci.* **1992**, *32* (17), 1261–1263. (e) Nesterov, A. E.; Lipatov, Y. S.; Horichko, V. V.; Gritsenko, O. T. *Polymer* **1992**, *33* (3), 619–622. (f) Nesterov, A. E.; Lipatov, Y. S. *Polymer* **1999**, *40* (5), 1347–1349.
(8) Karim, A.; Liu, D. W.; Douglas, J. F.; Nakatani, A. I.; Amis, E. J. *Polymer* **2000**, *41* (23), 8455–8458.
(9) Gomez, C. M.; Porcar, I.; Monzo, I. S.; Abad, C.; Campos, A. *Eur. Polym. J.* **2007**, *43* (2), 360–373.
(10) Ginzburg, V. V. *Macromolecules* **2005**, *38* (6), 2362–2367.
(11) Ginzburg, V. V.; Qiu, F.; Paniconi, M.; Peng, G. W.; Jasnow, D.; Balazs, A. C. *Phys. Rev. Lett.* **1999**, *82* (20), 4026–4029.
(12) Yurekli, K.; Karim, A.; Amis, E. J.; Krishnamoorti, R. *Macromolecules* **2003**, *36* (19), 7256–7267.
(13) Chung, H.; Ohno, K.; Fukuda, T.; Composto, R. J. *Nano Lett.* **2005**, *5* (10), 1878–1882.
(14) Chung, H.; Ohno, K.; Fukuda, T.; Composto, R. J. *Macromolecules* **2007**, *40* (2), 384–388.
(15) Chung, H. J.; Taubert, A.; Deshmukh, R. D.; Composto, R. J. *Europhys. Lett.* **2004**, *68* (2), 219–225.
(16) Peng, G. W.; Qiu, F.; Ginzburg, V. V.; Jasnow, D.; Balazs, A. C. *Science* **2000**, *288* (5472), 1802–1804.
(17) (a) Wong, H. C.; Sanz, A.; Douglas, J. F.; Cabral, J. T. *J. Mol. Liq.* **2010**, *153*, 79–87. (b) Wong, H. C.; Cabral, J. T. *Phys. Rev. Lett.* **2010**, *105*, 038301.
(18) Sanz, A.; Wong, H. C.; Douglas, J. F.; Cabral, J. T. Submitted for publication.
(19) Kropka, J. M.; Sakai, V. G.; Green, P. F. *Nano Lett.* **2008**, *8* (4), 1061–1065.
(20) Oh, H.; Green, P. F. *Nat. Mater.* **2009**, *8* (2), 139–143.
(21) Bansal, A.; Yang, H. C.; Li, C. Z.; Cho, K. W.; Benicewicz, B. C.; Kumar, S. K.; Schadler, L. S. *Nat. Mater.* **2005**, *4* (9), 693–698.
(22) Cabral, J. T.; Higgins, J. S. *Macromolecules* **2009**, *42* (24), 9528–9536.
(23) Mackay, M. E.; Tuteja, A.; Duxbury, P. M.; Hawker, C. J.; Van Horn, B.; Guan, Z. B.; Chen, G. H.; Krishnan, R. S. *Science* **2006**, *311* (5768), 1740–1743.
(24) Tuteja, A.; Duxbury, P. M.; Mackay, M. E. *Macromolecules* **2007**, *40* (26), 9427–9434.
(25) Waller, J. H.; Bucknall, D. G.; Register, R. A.; Beckham, H. W.; Leisen, J.; Campbell, K. *Polymer* **2009**, *50* (17), 4199–4204.
(26) Sariciftci, N. S.; Smilowitz, L.; Heeger, A. J.; Wudl, F. *Science* **1992**, *258* (5087), 1474–1476.
(27) Kim, C. K.; Paul, D. R. *Macromolecules* **1992**, *25* (12), 3097–3105.
(28) Mackay, M. E.; Dao, T. T.; Tuteja, A.; Ho, D. L.; Van Horn, B.; Kim, H. C.; Hawker, C. J. *Nat. Mater.* **2003**, *2* (11), 762–766.
(29) Anderson, B. J.; Zukoski, C. F. *Macromolecules* **2009**, *42* (21), 8370–8384.
(30) Wisniewsky, C.; Marin, G.; Monge, P. *Eur. Polym. J.* **1984**, *20* (7), 691–695.
(31) Londono, J. D.; Narten, A. H.; Wignall, G. D.; Honnell, K. G.; Hsieh, E. T.; Johnson, T. W.; Bates, F. S. *Macromolecules* **1994**, *27* (10), 2864–2871.
(32) Kim, C. K.; Paul, D. R. *Polymer* **1992**, *33* (8), 1630–1639.
(33) Binder, K.; Frisch, H. L.; Jackle, J. *J. Chem. Phys.* **1986**, *85* (3), 1505–1512.
(34) de Gennes, P.-G., *Scaling Concepts in Polymer Physics*. Cornell University Press: Ithaca, NY, 1979.
(35) Schultz, G. V. *Z. Phys. Chem. Abt. B* **1939**, *43*, 25.
(36) Zimm, B. H. *J. Chem. Phys.* **1948**, *16*, 1099.
(37) Higgins, J. S.; Benoit, H. C., *Polymers and Neutron Scattering*; Clarendon Press: Oxford, U.K., 1994.
(38) $G'' = 1.101/T - 0.00209$, as compared to $G'' = 1.164/T - 0.00223$ in ref 22. However, the M_w of the PSd in ref 22 is 225 000 g/mol, in contrast to 100 300 g/mol in the present work.
(39) Strobl, G., *The Physics of Polymers*; Springer-Verlag: Berlin, 1996.
(40) Balsara, N. P. Thermodynamics of Polymer Blends. In *Physical Properties of Polymers Handbook*; Mark, J. E., Ed.; AIP Press: Melville, NY, 1996; pp 257−268.
(41) Merfeld, G. D.; Paul, D. R. *Polymer* **2000**, *41* (2), 649–661.
(42) Koningsveld, R.; Stockmayer, W. H.; Nies, E., *Polymer Phase Diagrams*; Oxford University Press: Oxford, U.K., 2001.
(43) Dudowicz, J.; Freed, K. F.; Douglas, J. F. *Macromolecules* **1995**, *28* (7), 2276–2287.
(44) Kim, J. K.; Jang, J.; Lee, D. H.; Ryu, D. Y. *Macromolecules* **2004**, *37* (23), 8599–8605.
(45) Timmermans, J. *Z. Phys. Chem.* **1907**, *58*, 129–131.
(46) Cohn, R. H.; Jacobs, D. T. *J. Chem. Phys.* **1984**, *80* (2), 856–859.
(47) Hales, B. J.; Bertrand, G. L.; Hepler, L. G. *J. Phys. Chem.* **1966**, *70* (12), 3970–3975.
(48) Brannock, G. R.; Paul, D. R. *Macromolecules* **1990**, *23* (25), 5240–5250.
(49) Kim, C. K.; Kim, J. J.; Paul, D. R. *Polym. Eng. Sci.* **1994**, *34* (24), 1788–1798.